# Stoichiometry and Defect Structure Control in the Ternary Lithium Nitridometalates $Li_{3-x-y}Ni_xN$

Zlatka Stoeva,[†] Ronald I. Smith,[‡] and Duncan H. Gregory*,[†]

*School of Chemistry, University of Nottingham, Nottingham, NG7 2RD U.K., and ISIS Facility, Rutherford Appleton Laboratory, Chilton, Didcot, OX11 0QX U.K.*

*Received July 26, 2005. Revised Manuscript Received November 8, 2005*

A comprehensive study of the system $Li_{3-x-y}Ni_xN$ has investigated systematically the way in which synthesis parameters can be utilized to control stoichiometry and structure. Powder neutron diffraction and SQUID magnetometry have been used to characterize several representative compounds (with $0 < x < 1$) in the ternary phase system. The results show that processing conditions such as reaction time and temperature have profound effects on the levels of lithium vacancies ($y$) that, in a manner similar to lithium nitride ($Li_3N$) itself, are randomly distributed across lithium sites within the hexagonal [$Li_{2-y}N$] planes. Nickel occupies the interplanar site with lithium irrespective of the doping level, $x$, or the synthesis conditions applied. The magnetic behavior evolves from localized Curie−Weiss-type to delocalized Pauli paramagnetic with increased nickel substitution levels. The concentration of lithium vacancies, however, appears to have no profound effect on the magnetic and electronic properties. The results suggest that increasing $y$ at constant $x$ most probably leads to the formation of holes in bands with nitrogen 2p character rather than in localized nickel 3d bands.

## Introduction

The lithium nitridometalates $Li_{3-x-y}M_xN$ (M = Cu, Co, Ni; $y$= vacancy) have emerged as promising candidates for anode materials in lithium ion batteries.[1,2] These compounds have been known for a long time, and their synthesis and structures were reported as early as 1949 by Juza et al.,[3] although, at that time, the existence of vacancies ($y > 0$) was not established. The lithium nitridometalates are isostructural with the binary nitride $Li_3N$ in which the interplanar Li(1) site is partially occupied by a transition metal atom. This substitution has important consequences for the physical properties and underpins the application of the ternary nitrides as electrode materials, in contrast to the parent compound $Li_3N$, which displays essentially electrolytic properties.

In view of the application of ternary nitridometalates, it is now timely to understand in more detail their structures and structure−property relations. In this context, the ion-transport properties and electronic conductivity are among the most important characteristics, and these, in turn, are determined by the crystal structures. Although the basic structural features of the $Li_{3-x-y}M_xN$ compounds are relatively well-established, little work has been done on establishing some essential structural details such as the levels of lithium ion vacancies and how these might be controlled. The numbers of lithium ion vacancies are important because they influence the ion-transport properties and the nominal oxidation state of the transition metal. It should be noted here that ion transport in the parent compound $Li_3N$ takes place by a vacancy mechanism and 1−2% of lithium ion vacancies within the [$Li_{2-y}N$] planes are responsible for the unusually high ionic conductivity. It would be intriguing to determine whether similar structure−property relationships can be found in the ternary nitridometalates.

There has been some discussion in the literature regarding the defect chemistry in the ternary nitrides and the numbers of lithium vacancies in particular. In our previous neutron diffraction investigation of the ternary nitridonickelate $Li_{1.36}Ni_{0.79}N$,[4] we found that this compound contains 43% lithium vacancies randomly distributed within the [$Li_{2-y}N$] planes. These results corroborate our recent investigation of a series of ternary nitridometalates $Li_{3-x-y}M_xN$ (M = Cu, Ni, Co) that found fast lithium ion diffusion and, in some cases, improved diffusion parameters as compared to the parent compound $Li_3N$.[5,6] In contrast, Niewa et al. reported much lower vacancy concentrations ($\leq$ 1%) on the basis of their X-ray diffraction data, thermal measurements, and chemical analysis.[7] To establish the causes for these differences and understand better the role of the structural defects in the physical properties and electrochemical performance of the lithium nitridometalates, we have performed a detailed study of the relationship between synthetic methods and structural

* To whom correspondence should be addressed. E-mail: Duncan.Gregory@nottingham.ac.uk. Fax: 0115 951 3563. Tel.: 0115 951 4594.
[†] University of Nottingham.
[‡] Rutherford Appleton Laboratory.

(1) Nishijima, M.; Kagohashi, T.; Imanishi, M.; Takeda, Y.; Yamamoto, O.; Kondo, S. *Solid State Ionics* **1996**, *83*, 107.
(2) Shodai, T.; Okada, S.; Tobishima, S.; Yamaki, J. *Solid State Ionics* **1996**, *86*−*88*, 785.
(3) Sachsze, W.; Juza, R. *Z. Anorg. Allg. Chem.* **1949**, *259*, 278.
(4) Gregory, D. H.; O'Meara, P. M.; Gordon, A. G.; Hodges, J. P.; Short, S.; Jorgensen, J. D. *Chem. Mater.* **2002**, *14*, 2063.
(5) Stoeva, Z.; Gomez, R.; Allan, M.; Gordon, A. G.; Gregory, D. H.; Hix, G. B.; Titman, J. J. *J. Am. Chem. Soc.* **2004**, *126*, 4066.
(6) Stoeva, Z.; Gomez, R.; Gregory, D. H.; Hix, G. B.; Titman, J. J. *Dalton Trans.* **2004**, *19*, 3093.
(7) Niewa, R.; Huang, Z.-L.; Schnelle, W.; Hu, Z.; Kniep, R. *Z. Anorg. Allg. Chem.* **2003**, *629*, 1778.

10.1021/cm051644e CCC: $33.50 
Published on Web 12/16/2005

defects in several representative $Li_{3-x-y}Ni_xN$ samples. Accurate structure parameters were obtained from powder neutron diffraction data. Neutron diffraction was the technique of choice in this work because it allows reliable information to be obtained regarding the distribution and levels of lithium vacancies in the structure. Further, neutron diffraction data are collected using large amounts of bulk samples, similar to the amounts used in electrochemical tests. In this way, erroneous results caused by local inhomogeneities or impurities in the samples are significantly minimized. As a result of this investigation, we have established methods to control and tune the structural defects in the $Li_{3-x-y}Ni_xN$ compounds and, correspondingly, some of the crucial physical properties of these materials.

## Experimental Section

Because of air and moisture sensitivity, all starting materials and products were handled in an inert atmosphere (Saffron Scientific, $N_2$-filled recirculating glovebox; $O_2 < 1$ ppm, $H_2O < 5$ ppm) at all times unless otherwise indicated. The binary compound $Li_3N$ was synthesized by reaction of molten lithium−sodium alloy with dried nitrogen at 450 °C for 3−4 days. Cleaned Li metal (Alfa, >99%) was added initially to molten sodium (Aldrich, 99.95%) in an Ar-filled evacuable glovebox to form the alloy. Sodium is used as an inert solvent in this reaction and is subsequently removed by vacuum distillation at 400−450 °C for 24 h. The product, a highly crystalline purple powder, was identified as single-phase $Li_3N$ using powder X-ray diffraction (PXD) by comparison to the ICDD PDF database (Card No. 30-759).

For the preparation of each ternary nitride, a mixture of $Li_3N$ and nickel powder (Alfa, 99.9%) of predetermined molar ratio was thoroughly ground and pressed into a pellet, which was loaded directly into an alumina crucible and then sealed in a stainless steel reaction vessel under $N_2$ gas at ambient pressure and heated at 853 or 963 K. Most preparations involved intermittent regrinding and repelleting of the reaction mixture. The ternary nitride products were dark green/black powders, and these were initially analyzed by PXD. The samples obtained in this way were of very high purity, and only in isolated cases could small amounts of $Li_2O$ be detected. No traces of nickel metal impurities were found in the X-ray diffraction patterns. Further, there was no direct evidence of any reaction between the pellets and the alumina crucibles, and no known impurities (other than, occasionally, $Li_2O$ as noted above) or unidentified phases were detected in the ternary nitride products by PXD (see below).

Preliminary work on the synthesis of the ternary nitridonickelates and characterization by PXD showed that the reaction temperature and duration were important factors that appeared to regulate the structure of the products. It was established that the reactions did not take place at temperatures below ca. 830 K, whereas above 1000 K, we observed $Li_3N$ loss and/or ternary phase decomposition and the nickel metal phase separated. Similarly, Niewa et al. reported the formation of metallic nickel and decomposition of the products above 970 K.[7] Regarding the reaction times, prolonged annealing was necessary to complete the reactions at 853 K. At this temperature, reaction times shorter than 4−5 days resulted in significant amounts of starting materials remaining unreacted.

Following these preliminary observations, six representative samples were prepared using strictly controlled synthetic conditions. Three of these samples were synthesized at 963 K, and two were prepared at 853 K. The reactions times were 7 days with the exception of one sample, which was heated for 24 h only. Heating and cooling rates of 2 K $min^{-1}$ were used in all cases. The present work focused principally on two doping levels ($x$) that are similar to the compositions of the nitride anode materials studied by other authors,[1,2] and therefore some comparisons and conclusions regarding the electrochemical performance can be drawn. For comparison, the results for a sample of higher nickel doping are also presented and discussed. The latter sample was obtained at 983 K. For high nickel concentrations ($x > 0.6$), higher reaction temperatures (973 K and above) were found to be necessary to ensure complete reaction. Lower preparation temperatures in this case resulted in some amount of nickel metal remaining unreacted, as evidenced by PXD and the magnetic response of the samples. Intermediate regrindings were also essential to produce ternary nitrides with high nickel doping levels. The preparation conditions for each of the six samples are summarized in Table 1.

**Table 1. Description of the Samples Used in the Present Investigation**

| sample | reaction temperature (K) | reaction time (h) | nominal value of $x$ |
|---|---|---|---|
| **1** | 963 | 168 | 0.40 |
| **2** | 963 | 24 | 0.40 |
| **3** | 853 | 168 | 0.40 |
| **4** | 963 | 168 | 0.60 |
| **5** | 853 | 168 | 0.60 |
| **6** | 983 | 168 | 0.75 |

**Powder X-ray Diffraction.** PXD data were collected on a Philips XPERT $\theta-2\theta$ diffractometer with Cu K$\alpha$ radiation. Because of air and moisture sensitivity, the samples were sealed in custom-designed sample holders during data collection.[8] Phase purity was assessed from 2-h scans over the range 5−100° $2\theta$ using the Philips PC−IDENTIFY routine to access the PDF database and by further cross-referencing to powder patterns generated from the Inorganic Crystal Structure Database (ICSD) using Powdercell 3.[9] Indexing was performed using DICVOL91,[10] and/or cell parameters were refined by least-squares fitting from known reflections (in hexagonal space group $P6/mmm$ by analogy to $Li_3N$). Extended scan times of up to 12 h were used to obtain data suitable for Rietveld refinement. Strong preferred orientation effects were evident in the powder patterns, and in some cases, some hydrolysis of samples over the course of the diffraction experiment was observed. Coupled with the inherent difficulties in using PXD to locate light atoms such as Li, this made extraction of accurate structural models by Rietveld refinement against PXD data difficult. Notably, although reasonable models for the structures could be obtained [including location and quantification of Ni on the Li(1) site], reliable Li fractional occupancies for the two lithium sites—particularly that of the intraplanar Li(2) site—were not forthcoming. Therefore, neutron diffraction data, as discussed below, were used to obtain detailed and precise structural information.

**Powder Neutron Diffraction.** Time-of-flight (TOF) powder neutron diffraction (PND) data were collected using the high-intensity diffractometer POLARIS at the ISIS spallation source, Rutherford Appleton Laboratory, U.K. The powder samples, ca. 1.5−2 g each, were sealed into thin-walled vanadium cans in a $N_2$-filled glovebox, and the cans loaded into a helium cryostat (AS Scientific Instruments, Abingdon, U.K.). Neutron diffraction data were collected at 250 K using the three fixed detector banks consisting of either $^3$He gas tubes at $\langle 2\theta \rangle = 35°$ and $\langle 2\theta \rangle = 145°$ or a ZnS scintillator at $\langle 2\theta \rangle = 90°$. The temperature of the samples was monitored using a RhFe sensor attached to the outside wall of

(8) Barker, M. G.; Begley, M. J.; Edwards, P. P.; Gregory, D. H.; Smith, S. E. *J. Chem. Soc., Dalton Trans.* **1996**, *1*, 1.
(9) Nolze, G.; Kraus W. *Powder Diffr.* **1998**, *13*, 256.
(10) Boultif, A.; Louer, D. *J. Appl. Crystallogr.* **1991**, *24*, 987.

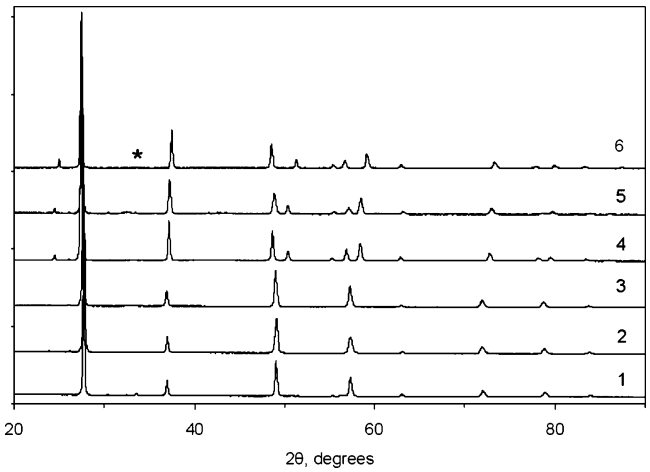


**Figure 1.** Powder X-ray diffraction patterns of the six representative samples $Li_{3-x-y}Ni_xN$ (labeled 1−6), which were subsequently submitted for powder neutron diffraction experiments and magnetic measurements. The asterisk indicates the position of the observed reflection from $Li_2O$.

the vanadium sample cans. Rietveld refinement against PND data was performed using the General Structure Analysis System (GSAS).[11] Data from all three detector banks were used simultaneously in the final least-squares cycles for each sample. The structure of α-$Li_3N$ in hexagonal space group *P*6/*mmm* in which nickel atoms partially substitute at the interplanar Li(1) site (0, 0, $^1/_2$) was taken as an initial model. This model was considered a reasonable starting point taking into account our PXD data, described above, and the results of our previous studies for similar phases using single-crystal X-ray diffraction.[12] At the outset of the refinements, fractional occupancies were taken from the nominal compositions used in the preparations. The Li(2) sites were initially treated as fully occupied. Peak shapes were modeled using the type-3 profile function in GSAS, which is a convolution of back-to-back exponentials with a pseudo-Voigt function. Initial cycles allowed for the variation of the scale factor, background coefficients to model high- and low-*Q* contributions (function type 6 within GSAS), and lattice parameters. As the refinements progressed, peak profile parameters and absorption coefficients were introduced. Anisotropic thermal parameters and site occupancy factors were refined in final cycles. No impurity phases were detected in the PND data. The small amounts of oxide impurities occasionally found in the PXD data probably resulted from oxidation during data collection. The vanadium sample can and the vacuum windows in the cryostat yielded a group of reflections that were excluded from the refinements. These excluded regions did not contain reflections arising from the compounds under study.

**Magnetic Measurements.** Magnetic susceptibility measurements were performed in the temperature range 5−250 K with a Quantum Design MPMS XL 5T SQUID susceptometer. The samples were loaded into airtight gelatine capsules in an inert atmosphere ($N_2$ glovebox). All data presented here were collected at an applied magnetic field of 1000 Oe and were corrected for the diamagnetic contributions from the gelatine sample containers.

## Results and Discussion

**Structure Refinements.** Examination of the peak positions in the X-ray diffraction patterns, shown in Figure 1, and subsequent indexing confirmed that all samples are isostructural with the parent binary compound $Li_3N$. This result is in agreement with previous studies of lithium nitridonickelates of similar compositions that found that the structures of these compounds closely resemble that of α-$Li_3N$.[3−4,7] Therefore, Rietveld refinements against neutron data were performed using a structural model based on the crystal structure of α-$Li_3N$ in space group *P*6/*mmm* in which the nickel atoms substitute at the interplanar Li(1) site (0, 0, $^1/_2$) as discussed in the Experimental Section above.

All refinements performed as described above produced very good fits to the experimental data, suggesting that the final refined structures were correct. Rietveld refinements were also attempted for a structural model in which the nickel atoms substitute at the intraplanar Li(2) site. Such a possibility was suggested from X-ray absorption studies, which found that, at low *x* ($x = 0.06$), the metal atoms are statistically distributed over the Li(2) positions.[7] However, fractional occupancies at the Li(2) site in these refinements converged to values higher than 1, suggesting that this model was incorrect. Nevertheless, it is possible that metal substitution at the Li(2) site takes place only for very small values of *x*.

The neutron diffraction and X-ray diffraction data gave no evidence for long-range ordering of either nickel atoms at the Li(1) site or lithium atoms (vacancies) at the Li(2) site. Such ordering could be demonstrated by the appearance of additional supercell reflections in the diffraction patterns. No such reflections were observed in any of our patterns. Synchrotron powder X-ray diffraction data collected at the SRS, Daresbury Laboratory, Daresbury, U.K. (not discussed here), also confirmed the absence of any additional reflections and hence ruled out the possibility of supercell formation. It can be concluded that the ternary nitridometalates $Li_{3-x-y}Ni_xN$ are completely disordered in terms of lithium/nickel distribution at the interplanar (0, 0, $^1/_2$) site and lithium/vacancy distribution at the interplanar ($^1/_3$, $^2/_3$, 0) site. The final structural parameters obtained from neutron diffraction data are listed in Tables 2−4. The structure of the $Li_{3-x-y}Ni_xN$ compounds is shown in Figure 2, and representative examples of the profile fits are given in Figure 3.

**Crystal Structures.** The structures determined from neutron diffraction data in this work agree with previous reports and have provided precise determinations of the crystallographic parameters, given the usual conditions and estimation of errors in Rietveld refinement.[13] The data demonstrate that the structural basis of the ternary $Li_{3-x-y}Ni_xN$ compounds is that of the parent compound α-$Li_3N$.[3−4,7] The space group remains the same as in α-$Li_3N$ (*P*6/*mmm*). Nickel atoms substitute at the interplanar Li(1) site, whereas lithium ion vacancies resulting from aliovalent substitution are distributed within the [$Li_{2-y}N$] planes. Similarly to previous reports from X-ray diffraction studies,[3,7] increasing nickel substitution levels (*x*) lead to the shortening of the *c* parameter and an increase in the *a* parameter. The nitrogen and the lithium [Li(2)] atoms within the [$Li_{2-y}N$] planes are in hexagonal bipyramidal and trigonal planar coordination, respectively. In all cases, the interplanar nickel/lithium atoms [Li(1)] are linearly coordinated to two nitrogen atoms. The

(11) Larson, A. C.; von Dreele, R. B. *The General Structure Analysis System*; Report LAUR 086-748; Los Alamos National Laboratories (LANL): Los Alamos, NM, 2000.

(12) Gordon, A. G.; Smith, R. I.; Wilson, C.; Stoeva, Z.; Gregory, D. H. *Chem. Commun.* **2004**, 2812.

(13) David, W. I. F. *J. Appl. Crystallogr.* **2004**, *37*, 621.

**Table 2. Crystallographic Parameters Obtained from Powder Neutron Diffraction at 250 K**

| instrument, radiation | POLARIS ToF diffactometer, neutron | | | | | |
|---|---|---|---|---|---|---|
| sample | $Li_{3-x-y}Ni_xN$ (**1**) | $Li_{3-x-y}Ni_xN$ (**2**) | $Li_{3-x-y}Ni_xN$ (**3**) | $Li_{3-x-y}Ni_xN$ (**4**) | $Li_{3-x-y}Ni_xN$ (**5**) | $Li_{3-x-y}Ni_xN$ (**6**) |
| *x* | 0.362(2) | 0.339(1) | 0.360(1) | 0.565(2) | 0.577(3) | 0.743(6) |
| *y* | 0.320(14) | 0.126(8) | 0.162(9) | 0.412(11) | 0.188(8) | 0.626(9) |
| crystal system | hexagonal | | | | | |
| space group | *P*6/*mmm* | | | | | |
| *Z* | 1 | | | | | |
| *M* | 51.364 | 51.496 | 52.340 | 61.187 | 63.366 | 68.960 |
| *a* parameter (Å) | 3.70773(7) | 3.70529(3) | 3.70812(5) | 3.73350(3) | 3.73283(4) | 3.76044(5) |
| *c* parameter (Å) | 3.7108(10) | 3.72034(7) | 3.7036(10) | 3.61302(4) | 3.61281(6) | 3.53256(7) |
| unit cell volume ($Å^3$) | 44.179(1) | 44.234(1) | 44.102(1) | 43.615(1) | 43.597(1) | 43.261(1) |
| calculated density, $\rho_X$ (g $cm^{-3}$) | 1.931 | 1.933 | 1.971 | 2.330 | 2.414 | 2.647 |
| observations, parameters | 13769, 62 | 13486, 62 | 13484, 62 | 13885, 62 | 13886, 62 | 15087, 62 |
| $R_p$ | 0.0199 | 0.0235 | 0.0232 | 0.0251 | 0.0198 | 0.0261 |
| $R_{wp}$ | 0.0108 | 0.0139 | 0.0141 | 0.0147 | 0.0105 | 0.0171 |
| $\chi^2$ | 1.169 | 1.938 | 2.153 | 1.716 | 1.103 | 2.773 |

**Table 3. Refined Atomic Parameters Obtained from Powder Neutron Diffraction**

| sample | **1** | **2** | **3** | **4** | **5** | **6** |
|---|---|---|---|---|---|---|
| synthesis temperature (K) | 963 | 963 | 853 | 963 | 853 | 983 |
| reaction time (h) | 168 | 24 | 168 | 168 | 168 | 168 |
| | | | (Li,Ni)(1) (0, 0, 0.5) | | | |
| Ni occupancy | 0.362(2) | 0.339(1) | 0.360(1) | 0.565(2) | 0.577(3) | 0.743(6) |
| $U_{11} = U_{22}$ | 0.0057(6) | 0.0065(4) | 0.0043(5) | 0.0165(3) | 0.0173(6) | 0.0232(3) |
| $U_{33}$ | 0.028(2) | 0.028(1) | 0.024(1) | 0.0081(5) | 0.0108(9) | 0.0082(3) |
| $U_{12}$ | 0.0028(3) | 0.0033(2) | 0.0021(2) | 0.0083(2) | 0.0086(3) | 0.0116(2) |
| | | | Li(2)(0.3333, 0.6667, 0) | | | |
| occupancy | 0.842(14) | 0.937(8) | 0.919(9) | 0.794(11) | 0.906(8) | 0.687(9) |
| $U_{11} = U_{22}$ | 0.015(1) | 0.0203(7) | 0.0141(8) | 0.030(1) | 0.024(1) | 0.024(2) |
| $U_{33}$ | 0.102 (5) | 0.091(2) | 0.093(3) | 0.070(2) | 0.075(3) | 0.084(4) |
| $U_{12}$ | 0.0073(6) | 0.0102(3) | 0.0071(4) | 0.0148(5) | 0.0121(7) | 0.0118(9) |
| | | | N (0, 0, 0) | | | |
| occupancy | 1 | 1 | 1 | 1 | 1 | 1 |
| $U_{11} = U_{22}$ | 0.0199(3) | 0.0195(2) | 0.0157(2) | 0.0251(3) | 0.0246(4) | 0.0275(3) |
| $U_{33}$ | 0.0242(6) | 0.0285(3) | 0.0217(5) | 0.0237(4) | 0.0213(8) | 0.0203(3) |
| $U_{12}$ | 0.0100(2) | 0.00976(8) | 0.0079(1) | 0.0125(1) | 0.0123(2) | 0.0137(2) |

**Table 4. Selected Interatomic Distances and Angles Obtained from Rietveld Refinements**

| | sample | | | | | |
|---|---|---|---|---|---|---|
| atomic distance or angle | **1** | **2** | **3** | **4** | **5** | **6** |
| (Li,Ni)(1)−N×2 (Å) | 1.85541(7) | 1.86017(4) | 1.85179(5) | 1.80651(2) | 1.80640(3) | 1.76628(3) |
| Li(2)−N×3 (Å) | 2.1406(2) | 2.1392(2) | 2.1408(2) | 2.1555(2) | 2.1550(2) | 2.1710(2) |
| Li(2)−Li(2) × 3, (Å) | 2.1406(2) | 2.1392(2) | 2.1408(2) | 2.1555(2) | 2.1550(2) | 2.1710(2) |
| (Li,Ni)(1)−Li(2) × 6 (Å) | 2.8328(1) | 2.8348(1) | 2.8306(1) | 2.8124(1) | 2.8120(1) | 2.7988(1) |
| (Li,Ni)(1)−N−(Li,Ni)(1) (deg) | 180 | 180 | 180 | 180 | 180 | 180 |
| Li(2)−N−Li(2) (deg) | 120 | 120 | 120 | 120 | 120 | 120 |

**Table 5. Bond Valence Calculations for Samples 1−6**

| | sample | | | | | |
|---|---|---|---|---|---|---|
| | **1** | **2** | **3** | **4** | **5** | **6** |
| (Li,Ni)(1) | 1.2 | 1.2 | 1.2 | 1.5 | 1.5 | 1.7 |
| Li(2) | 0.7 | 0.7 | 0.7 | 0.7 | 0.7 | 0.7 |
| N | −2.4 | −2.5 | −2.5 | −2.6 | −2.7 | −2.6 |

(Ni,Li)−N bond lengths and, correspondingly, the *c* parameter decrease with increasing nickel substitution because of the increased covalency of these bonds as less electropositive Ni replaces Li.

Examination of the data in Table 4 shows that the bond lengths depend mostly on *x*, whereas the variation of the bond lengths as a function of *y* at constant *x* is probably insignificant. The occupancy of the Li(2) site hence has a smaller effect on the interatomic distances and coordination chemistry at fixed *x* than variation of *x* itself. An important consequence of this fact is that the $Li_{3-x-y}Ni_xN$ compounds should exhibit good structural stability when the Li content in the crystal structure is varied. The latter is particularly relevant to the cycling properties of the nitride anode materials. This result corroborates electrochemical data obtained by other authors who found that the lattice parameters for the $Li_{2.5-z}Ni_{0.5}N$ phase vary only slightly with the discharge depth (*z*).[14] This behavior is in contrast to the ternary nitridocobaltates and -cuprates, which exhibit more significant changes in the lattice parameters on varying *z* and eventually lose long-range order and transform to amorphous materials.

The structural data listed in Tables 2 and 3 were used for bond valence calculations taking values from Brese and O'Keeffe[15] in order to obtain information about the site valences and, correspondingly, the charge balance mecha-

(14) Nishijima, M.; Kagohashi, T.; Takeda, Y.; Imanishi, M.; Yamamoto, O. *J. Power Sources* **1997**, *68*, 5106.

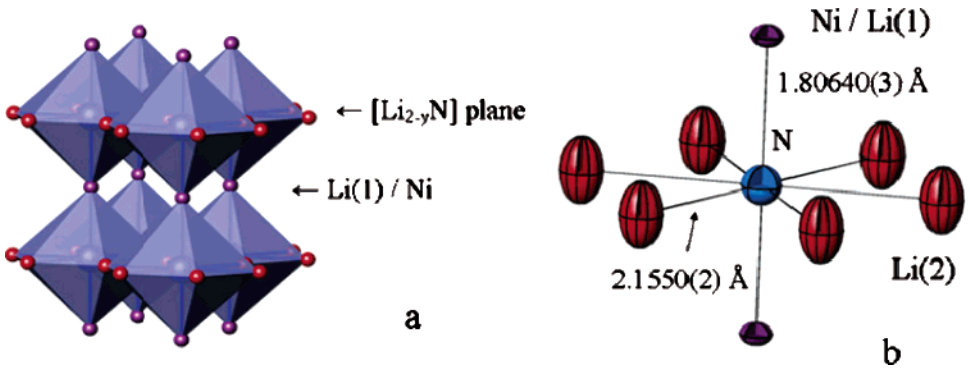


**Figure 2.** Structure of the Li−Ni−N compounds studied in this work. The drawings are based on the structural parameters obtained from PND at 250 K for sample 5. Nitrogen atoms are drawn in blue, and lithium atoms are drawn in red. The Li(1) atoms, partially replaced by nickel, are drawn in purple. (a) Polyhedral representation of the structure. (b) Coordination of the nitrogen atoms. Thermal ellipsoids are drawn at 50% probability.

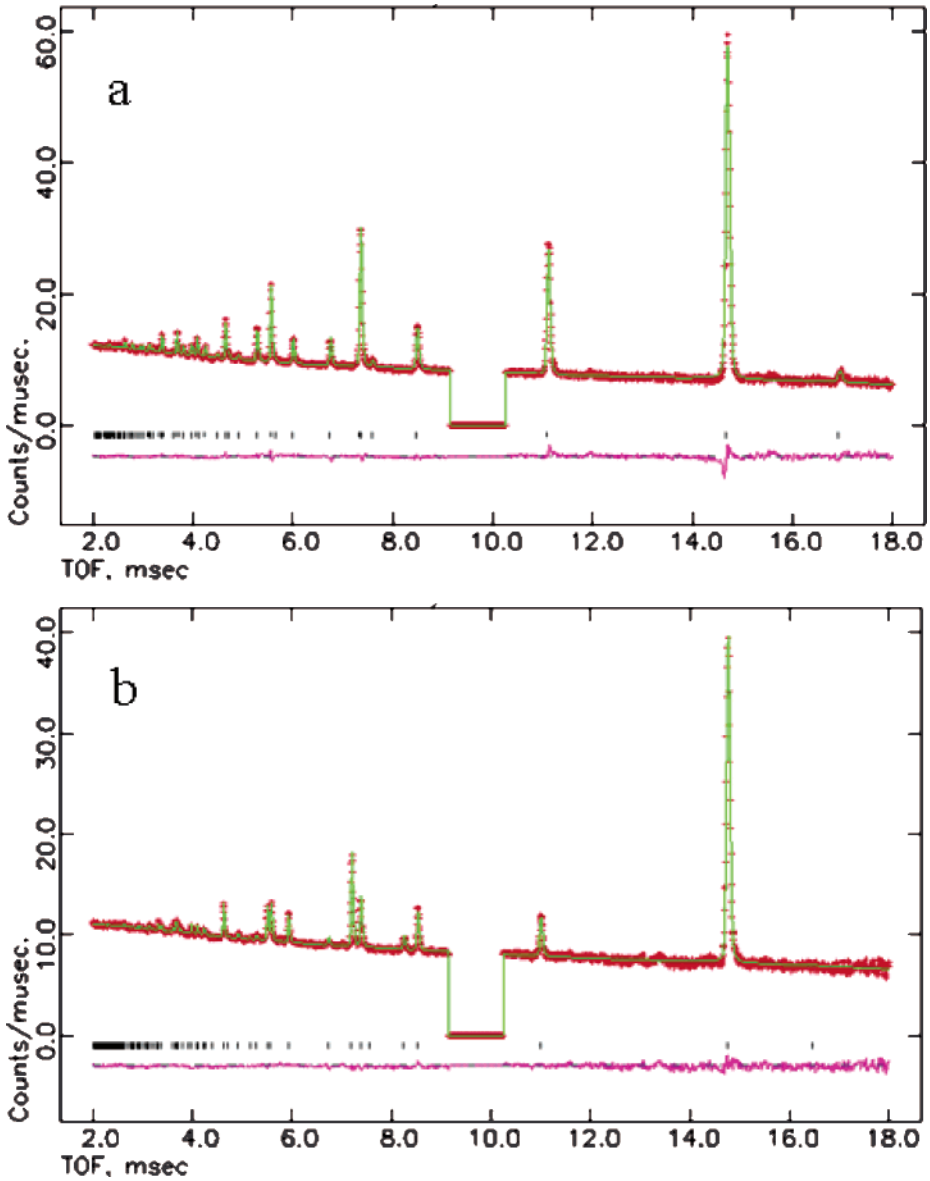


**Figure 3.** Observed, calculated, and difference profile plots for the Rietveld refinement against powder neutron diffraction data for (a) sample 3 and (b) sample **4** at 250 K. Crosses show the observed data points, solid lines represent the calculated diffraction patterns, and tick marks represent the calculated positions of the reflections. The data shown are from detectors at $<2\theta> = 90°$. Bragg reflections from the vanadium in the cryostat vacuum windows and the sample can are excluded from the refinements.

nism in the ternary nitrides, $Li_{3-x-y}Ni_xN$. The generated values are given in Table 5. These results should be treated with some caution, and for example, Li···Li interactions within the $[Li_{2-y}N]$ planes are not taken into account in the present calculations. Nevertheless, the calculations generate a semiquantitative description. The valence sum for the interplanar (Li,Ni) (1) site (0, 0, $^1/_2$) appears to depend mostly on the doping level $x$, whereas the dependence on $y$ at

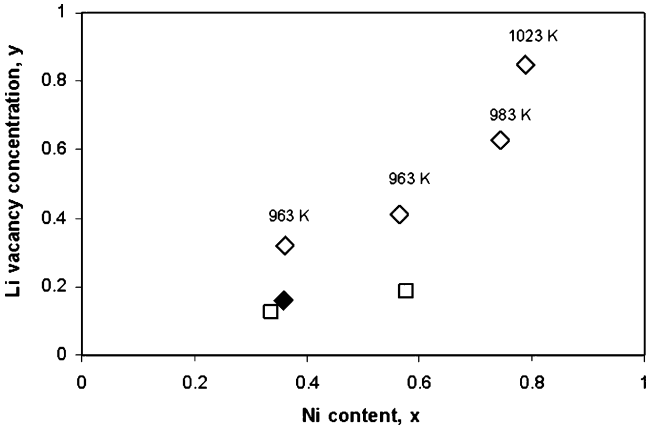


**Figure 4.** Relation of lithium vacancies concentration ($y$) to nickel doping level ($x$) at varying reaction temperatures. Open squares represent the samples heated at lower temperatures (853 K). Open diamonds show the "high-temperature" samples prepared at and above 963 K. The filled diamond represents the sample prepared at 963 K for the shorter reaction time.(24 vs 98 h). The data for the sample obtained at 1023 K is taken from ref 4. This latter sample was synthesized by a surface reaction on nickel metal foil (for 5 days) in contrast to the other samples, which were prepared by solid-state ceramic reactions. In all cases, the error bars for $x$ and $y$ are contained within the symbols.

constant $x$ is effectively negligible. The site valence increases significantly with $x$, broadly consistent with the idea of aliovalent substitution at the Li(1) site and the presence of $Ni^{2+}$. Perhaps most interesting, however, are the calculated valence sums for the N site, which appear to depend on $y$. Thus, the valence sum for nitrogen becomes less negative as the numbers of lithium vacancies ($y$) increases at approximately constant $x$, e.g., as is the case for compound **1** compared to compounds **2** and **3** and for compound **4** compared to **5**. The implications of this result is that nitrogen also plays a role in the charge balance process in the $Li_{3-x-y}Ni_xN$ compounds with the formation of holes on nitrogen (within N bands). These issues are discussed again below in view of the reported magnetic susceptibility data.

**Defect Structure.** The refined structural data listed in Tables 2 and 3 reveal that the preparation conditions have a major effect on the fractional occupancies at the intraplanar Li(2) site and, correspondingly, on the levels of the lithium ion vacancies in the ternary nitrides. The trends in the variation of vacancy concentrations ($y$) as a function of the preparation conditions also become apparent when plotted as in Figure 4. These trends can be summarized as follows: higher reaction temperatures result in lower occupancies at the Li(2) site and, correspondingly, larger numbers of $Li^+$ ion vacancies (e.g., sample **1** vs sample **3** and sample **4** vs sample **5**). Furthermore, for a fixed synthesis temperature, Li(2) site occupancy decreases and $Li^+$ vacancy concentration increases with extended reaction times (e.g., sample **1** vs sample **2**). The maximum numbers of vacancies were formed at high reaction temperatures (963 K and above) and long reactions times (6−7 days). These trends can be explained in terms of a loss of lithium that occurs as a result of increasing the reaction temperature. Hence, exerting a control over reaction temperature and duration mediates the amount of lithium that is lost from the ternary nitrides. However, it is likely that there is a critical limit of lithium content ($3 - x - y$) below which the compounds start to decompose and nickel metal starts to phase separate. No ternary phase in the Li−Ni−N system has yet been synthesized beyond LiNiN [i.e., $(x + y) > 2$]. We observe that, for samples that were heated in solid-state reactions above 1010−1020 K, significant amounts of $Li_3N$ sublime onto the upper (colder) walls of the reaction vessel, leading to strong deviations from the stoichiometry of the starting reaction mixture. In these cases, quantities of nickel metal are observed in powder products as a separate phase. It should be noted here that the sample shown in Figure 4 and synthesized at 1023 K was prepared by a surface reaction on a nickel foil in contrast to the samples studied in the present work.[4] The surface reactions allow higher temperatures to be used successfully in the preparation of ternary phases; however, they have not allowed as yet the controlled preparation of samples of low $x$ (below ~0.6). Regarding the reaction times, samples heated to an upper limit of 10 days at temperatures below 990 K yielded single-phase compounds, and no evidence of decomposition products was found in the X-ray diffraction patterns. It can also be seen from Figure 4 that the number of vacancies increases with increasing $x$, which supports the idea of aliovalent nickel substitution. The inference is that lithium vacancies are formed to maintain the charge balance following the substitution of $Ni^{2+}$ ions for the monovalent $Li^+$ ions.

It is intriguing to compare our results with data reported by other authors concerning defect chemistry in the ternary lithium nitridometalates. Shodai et al. reported the reaction mechanism of $Li_{3-x-y}Co_xN$ anode materials that were synthesized for a relatively short reaction time (8 h) at 873−1073 K.[16] In this case, apparently insignificant amounts of lithium vacancies were found as evidenced from chemical composition analysis and electrochemical tests. Similarly, Niewa et al. found that nitridocobaltate, -nickelate, and -cuprate samples synthesized for 20−40 h at 773−873 K contained negligible amounts of lithium vacancies.[7] The latter conclusions were made from Rietveld refinement using powder X-ray diffraction data and thermogravimetric and chemical analyses. These previous reports are consistent with the results presented here that show that short reaction times result in low levels of lithium ion vacancies. The only report in the literature of a $Li_3N$-derived nitridometalate synthesized at higher temperature is that of $Li_{2.2}Cu_{0.5}N$.[17] The nitridocuprate is formed at 973 K after 16 h under a $N_2$ pressure of 200 bar with a corresponding value of $y = 0.3$. Overall, the consistency observed in the available published data with our results seems to suggest strongly that there is a systematic relationship between synthetic conditions and numbers of lithium vacancies.

**Magnetic and Electronic Properties.** SQUID magnetic susceptibility measurements were used to determine how the magnetic and electronic properties of the ternary nitridometalates are affected by the preparation conditions. Because the preparation conditions influence the fractional occupan-

(15) Brese, N. E.; O'Keeffe, M. *Acta Crystallogr*. **1991**, *B47*, 192.
(16) Shodai, T.; Sakurai, Y.; Suzuki, T. *Solid State Ionics* **1999**, *122*, 85.
(17) Weller, M. T.; Dann, S. E.; Henry, P. F.; Currie, D. B *J. Mater. Chem.* **1999**, *9*, 283.

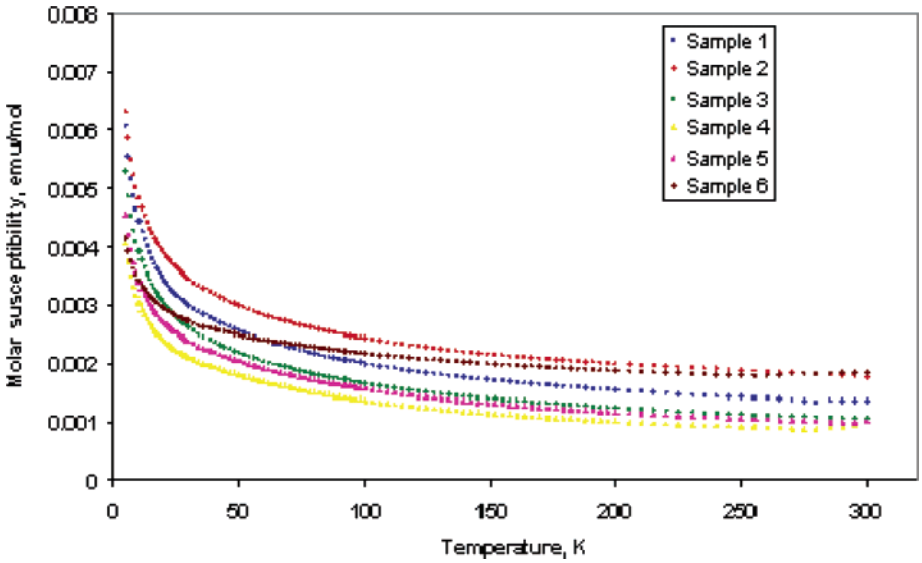


**Figure 5.** Plots of molar susceptibility vs temperature for samples 1−**6**.

**Table 6. Parameters Obtained from Fitting of Magnetic Susceptibility Data for 1−6**

| sample | $x$ | $y$ | $\chi_0$ | $C$ | $\theta$ (K) | $\mu_{eff}$ per Ni atom ($\mu_B$) |
|---|---|---|---|---|---|---|
| **1** | 0.362(2) | 0.320(14) | 0.00125(2) | 0.074(3) | −12.3(7) | 1.28 |
| **2** | 0.339(1) | 0.126(8) | 0.00168(2) | 0.078(3) | −13.7(7) | 1.36 |
| **3** | 0.360(1) | 0.162(9) | 0.00094(2) | 0.075(2) | −14.0(7) | 1.29 |
| **4** | 0.565(2) | 0.412(11) | 0.00077(2) | 0.063(3) | −16.9(9) | 0.95 |
| **5** | 0.577(3) | 0.188(8) | 0.00087(2) | 0.074(3) | −18.0(9) | 1.01 |
| **6** | 0.743(6) | 0.626(9) | 0.00196(2) | 0.079(3) | −18.4(9) | 0.79 |

cies at the Li(2) site, it can be expected that the corresponding loss of electrons will change the density of states at the Fermi level if there were a significant contribution from the Li(2) 2s band. The electronic structures of the ternary nitridometalates $Li_{3-x-y}Ni_xN$ have not been determined; however, reports suggest that the compounds of high $x$ display metallic conductivity.[7] This premise is in accord with our experimental observations for the $x = 1$ defect-ordered nitridonickelate LiNiN,[5] and similarly our DFT calculations for the $x = 1$ compound indicate the formation of a broad, partially filled band with contributions from N 2p and Ni 3d states.[18]

The temperature dependence of the magnetic susceptibility for the six samples studied in this work is shown in Figure 5. In all cases, the temperature dependence follows the modified Curie−Weiss law

$$\chi = \chi_0 + C/(T - \theta) \qquad (1)$$

where $\chi_0$ is a temperature-independent term, $C$ is the Curie constant, and $\theta$ is the Weiss constant. The effective magnetic moments and other parameters obtained from fitting the experimental data to eq 1 are given in Table 6.

The data in Table 6 show that there are only small variations in the magnetic properties of samples with fixed (similar) $x$ synthesized under different reaction conditions. Although there are some differences in the magnitude of the temperature-independent terms, the values for all samples are within the range $(770-1900) \times 10^{-6}$ emu mol$^{-1}$, which is characteristic of metallic Pauli paramagnetic behavior. The Weiss constant decreases slightly with increasing $x$, i.e., as the nickel fractional occupancy at the Li(1) site increases. This trend could be explained by the presence of local antiferromagnetic exchange interactions between the nickel atoms and has been previously observed by other authors.[7] The increasingly negative values of $\theta$ are due to increasing the length of the continuous $^1_\infty$[N−Ni] chains along the $c$-axis direction. The effective magnetic moment, $\mu_{eff}$, decreases with increasing substitution ($x$), consistent with progressive electron delocalization and appearance of metallic properties. In all cases, the values are smaller than the expected theoretical values for the spin-only magnetic moment for $Ni^+$ (1.72 $\mu_B$).

Compared with the magnetic susceptibility data for $Li_{3-x-y}Ni_xN$ compounds reported by Niewa et al.,[7] all $\mu_{eff}$ values obtained in our work are smaller for comparable substitution levels ($x$), and further, the Weiss constants are closer to zero. However, the trends in the variations are qualitatively similar to those reported in ref 7. The small differences are likely to arise from the distribution of the nickel atoms along the chains and local inhomogeneities, which will have a strong effect on the 1D magnetism and the ensuing magnetic parameters. Further studies, for example, by high-resolution electron microscopy, might shed some light on the variation of the physical properties with local structure.

The SQUID results suggest that the preparation conditions and the levels of $Li^+$ ion vacancies have only a small effect on the electronic properties of the ternary nitridonickelates. The electronic properties appear to be dominated by the levels of nickel doping rather than the occupancy of lithium at the Li(2) site. These results imply that the Li 2s states for the interplanar Li(2) site make only a small or negligible contribution to the density of states at the Fermi level.

The magnetic moments of the nickel atoms show small variations with varying Li(2) occupancy, but no particular trends become apparent. Were the moments more localized on Ni, one would expect an increase in $\mu_{eff}$ with $y$ commensurate with the aliovalent substitution of $Ni^{2+}$ for $Li^+$.

(18) Stoeva, Z.; Jäger, B.; Gomez, R.; Titman, J. J.; Messaoudi, S.; Ben Yahia, M.; Rocquefelte, X.; Gautier, R.; Wolf, W.; Herzig, P.; Gregory, D. H., manuscript in preparation.

It is possible, however, that the charge balance is maintained via the doping of holes in N 2p bands. Similar conclusions were made for $Li_{3-x-y}Co_xN$ compounds studied by core-level electron energy loss spectroscopy (EELS).[16,19] The latter studies have shown that the amount of holes introduced in the nitrogen 2p orbitals increases dramatically after electrochemical lithium extraction and is considered as evidence for increasing covalency between nickel and nitrogen. These results are consistent with our SQUID data and crystal chemical analysis and highlight the significant covalency effects within the Ni−N network. Again, the calculated electronic structure of LiNiN can be taken as a guide, and the contribution to the DOS at the Fermi level from Li 2s and 2p states in the ordered $x = 1$ nitride is relatively small.[18] Further studies of $Li_{3-x-y}Ni_xN$ compounds of different $y$ and $x$ values using XANES are currently underway. These studies are expected to provide further insight into the oxidation state of the nickel atoms and the mechanism of charge balance in these compounds.

**Implications for Electrochemical Performance.** The vacancy concentration and defect structure are important factors contributing to the electrochemical performance of the nitride anode materials in rechargeable lithium batteries. The lithium-rich phases (i.e., no lithium vacancies) cannot be directly combined with high-potential cathodes in order to obtain high-voltage lithium ion cells. For such high-voltage cells, the anode must be in its most oxidized state and the cathode in its most reduced state. Various approaches for optimizing the electrochemical properties of the nitride compounds have been reported. All of them involve various preliminary steps to control the lithium vacancy concentrations in the nitride-based anodes. For example, Takeda et al. used chemical pre-extraction to obtain lithium-poor ternary nitrides in order to obtain high-voltage batteries composed of a $Li_xCo_{0.4}N$ anode and a $Li_{1.1}Mn_{1.9}O_4$ cathode.[20] Similarly, Shodai et al. used electrochemical lithium extraction to obtain a $Li_{1.6}Co_{0.4}N$ anode material operating between 0 and 1.0 V and combined this with a high-voltage $LiNiO_2$ cathode.[21] The electrochemical cells constructed in this way showed good cycleability and a high specific capacity of about 500 mAh $g^{-1}$. A different approach was reported more recently by Liu et al., who prepared a composite anode by combining $Li_{2.6}Co_{0.4}N$ with $LiTi_2O_4$ and obtained large volumetric capacities of about 798 mAh $cm^{-3}$ and good cycling performance.[22] The role of $LiTi_2O_4$ in this case was to extract lithium from the ternary nitride and then function as an inert conducting material in the composite electrode.

Our results suggest that the preparation conditions themselves can be used to control the lithium vacancy concentrations without either the need of additional steps to pre-extract the lithium ions or the requirement of an additive to extract lithium in situ. It should be noted here that short preparation times (up to 12 h) were used in all of the above-mentioned previously reported electrochemical studies. Considering the results in the present investigation, such preparations are likely to produce low vacancy concentrations in the ternary nitridometalates. According to the results discussed here, appropriate synthetic conditions (high temperatures and longer reaction times) can be used to obtain ready-to-use electrode materials that have low lithium contents. Our preliminary results from electrochemical tests on ternary nitridometalates obtained at high temperatures and longer reaction times confirm the presence of significant numbers of lithium vacancies. We observe that these vacancies can be filled electrochemically in solid solution behavior and reversibly cycled from 0.95 to 0 V in reduction and from 0 to 1 V in oxidation.[23] Further detailed investigation of the electrochemical properties is currently in progress.

## Conclusions

In conclusion, we have established reproducible synthetic methods to obtain ternary lithium nitridonickellates $Li_{3-x-y}Ni_xN$ with controlled doping levels ($x$) and vacancy concentrations ($y$). Using powder neutron diffraction and SQUID magnetometry, we have found that the vacancy levels can be controlled by changing the reaction temperature and duration. The magnetic and electronic properties are influenced principally by the nickel substitution levels ($x$), and whereas $y$ has a small or negligible effect on these properties, the effect on $Li^+$ ionic conductivity is likely to be profound. The ability to control $x$ and $y$ and hence electronic and ionic conductivity in a systematic way is expected to have important implications for the application of these materials as anodes in lithium ion batteries. Clearly, high $Li^+$ ion mobility and high electronic conductivity are vital materials features for such applications. Although the exact relationship between lithium vacancy concentrations and $Li^+$ ion mobility in the $Li_{3-x-y}Ni_xN$ compounds is not known at this stage, it is not unreasonable to assume that the ternary nitridonickelates will behave similarly to the parent binary nitride, $Li_3N$. For the latter compound, molecular dynamics calculations have shown that diffusion within the $[Li_{2-y}N]$ planes is limited by the formation of $Li^+$ vacancies only. This is because of the extremely small energy barrier (0.004 eV) between vacant adjacent sites in the $[Li_{2-y}N]$ planes.[24] We are currently investigating these issues in more detail, including the effect of vacancy concentration on the mechanism and extent of $Li^+$ ion diffusion.

**Acknowledgment.** D.H.G. thanks the EPSRC (U.K.) for supporting this work (under Grant GR/R87345). The CCLRC (U.K.) is gratefully acknowledged for the award of beam time at ISIS.

CM051644E

(19) Suzuki, S.; Shodai, T.; Yamaki, J. *J. Phys. Chem. Solids* **1998**, *59* (3), 331.
(20) Takeda, Y.; Nishijima, M.; Yamahata, M.; Takeda, K.; Imanishi, N.; Yamamoto, O. *Solid State Ionics* **2000**, *130*, 61.
(21) Shodai, T.;.Okada, S.; Tobishima, S.; Yamaki, J. *J. Power Sources* **1997**, *68*, 515.
(22) Liu, Y.; Horikawa, K.; Fujiyoshi, M.; Matsumura, T.; Imanishi, N.; Takeda, Y. *Solid State Ionics* **2004**, *172*, 69.
(23) Stoeva, Z.; Cabana, J.; Palacin, R.; Gregory, D. H., manuscript in preparation.
(24) Sarnthein, J.; Schwarz, K.; Blöchl, P. E. *Phys. Rev. B* **1996**, *53* (14), 9084.